MONTANA
STATE UNIVERSITY

A computational model of two-phase, turbulent atmospheric boundary layers containing blowing snow
by Glen Eddy Liston

Abstract:
In blowing and drifting snow, two distinct flow regimes are found. At the surface is the saltation layer which, although very thin, is responsible for the majority of mass transport. Above this layer, the flow can be described as a turbulent, two-phase mixture of air and snow particles. These two layers are highly coupled, and therefore an accurate description of the general snow transport process requires a description of processes occurring within both of these layers.

A physically based computational model of the salient features of blowing and drifting snow in two-dimensional terrain is developed. The model has two distinct parts, one describing the turbulent flow mixture of air and snow, and a second describing the mass transport process and resulting snow accumulation patterns related to the saltation layer. The turbulent flow model consists of a general solution of the time averaged, two-dimensional Navier-Stokes equations, where the k-epsilon turbulence model is used to close the system of equations. The effect of particulates on the turbulent flow field is accounted for by computing the particle concentration field using a convection-diffusion equation and a subsequent modification of the k-epsilon model. The turbulent flow model is coupled to a saltation model and the time evolution of drift development and wind flow fields are computed.

The model suggests that, for the case of precipitating snow, snow particles can be considered a passive additive to the turbulent flow field. Modeled snow accumulation profiles are very similar to published field and experimental data.

A COMPUTATIONAL MODEL OF TWO-PHASE, TURBULENT

ATMOSPHERIC BOUNDARY LAYERS

CONTAINING BLOWING SNOW

by

Glen Eddy Liston

A thesis submitted in partial fulfillment
of the requirements for the degree

of

Doctor of Philosophy

in

Civil Engineering

MONTANA STATE UNIVERSITY
Bozeman, Montana

March 1991

ii

APPROVAL

of a thesis submitted by

Glen Eddy Liston

This thesis has been read by each member of the
thesis committee and has been found to be satisfactory
regarding content, English usage, format, citations,
bibliographic style, and consistency, and is ready for
submission to the College of Graduate Studies.

1 March 91
Date

R. L. Brown
Chairperson, Graduate Committee

Approved for the Major Department

26 Feb '91
Date

Theodore E. Long
Head, Major Department

Approved for the College of Graduate Studies

March 1, 1991
Date

Henry Parsons
Graduate Dean

STATEMENT OF PERMISSION TO USE

In presenting this thesis in partial fulfillment of
the requirements for a doctoral degree at Montana State
University, I agree that the Library shall make it
available to borrowers under rules of the Library. I
further agree that copying of this thesis is allowable
only for scholarly purposes, consistent with "fair use"
as prescribed in the U.S. Copyright Law. Requests for
extensive copying or reproduction of this thesis should
be referred to University Microfilms International, 300
North Zeeb Road, Ann Arbor, Michigan 48106, to whom I
have granted "the exclusive right to reproduce and
distribute copies of the dissertation in and from
microfilm and the right to reproduce and distribute by
abstract in any format."

Signature _____

Date _____1 March 1991_____

ACKNOWLEDGMENTS

I wish to express my sincere gratitude to Dr. Robert L. Brown for his unfailing support and guidance throughout this research effort. His willingness to allow me to develop my own direction and focus on my professional objectives has gone far towards making these past few years very successful. In addition, I would like to thank Drs. Bowers, Brown, Demetriades, Dent, Hansen, and Vogel for their instruction and consultation; they have all contributed to my educational and professional growth and success during my doctoral program at Montana State University.

This work was supported by the Center for High-Elevation Studies, the Department of Civil and Agricultural Engineering, and the Engineering Experiment Station at Montana State University.

TABLE OF CONTENTS

TABLE OF CONTENTS-<u>Continued</u>

LIST OF FIGURES

LIST OF FIGURES–<u>Continued</u>

ix

LIST OF FIGURES-<u>Continued</u>

ABSTRACT

In blowing and drifting snow, two distinct flow regimes are found. At the surface is the saltation layer which, although very thin, is responsible for the majority of mass transport. Above this layer, the flow can be described as a turbulent, two-phase mixture of air and snow particles. These two layers are highly coupled, and therefore an accurate description of the general snow transport process requires a description of processes occurring within both of these layers.

A physically based computational model of the salient features of blowing and drifting snow in two-dimensional terrain is developed. The model has two distinct parts, one describing the turbulent flow mixture of air and snow, and a second describing the mass transport process and resulting snow accumulation patterns related to the saltation layer. The turbulent flow model consists of a general solution of the time averaged, two-dimensional Navier-Stokes equations, where the k-epsilon turbulence model is used to close the system of equations. The effect of particulates on the turbulent flow field is accounted for by computing the particle concentration field using a convection-diffusion equation and a subsequent modification of the k-epsilon model. The turbulent flow model is coupled to a saltation model and the time evolution of drift development and wind flow fields are computed.

The model suggests that, for the case of precipitating snow, snow particles can be considered a passive additive to the turbulent flow field. Modeled snow accumulation profiles are very similar to published field and experimental data.

CHAPTER 1

INTRODUCTION

This document describes a study of the physical processes which govern blowing and drifting snow and the snow accumulation and distribution patterns which result from these processes. The study combines techniques from the fields of turbulence modeling, suspended and bed load transport, and computational fluid mechanics to describe the phenomenon of wind transported snow.

Outside our doors in the winter environment, whether it be in the city, the country, or the mountains, snow depth is found to be highly variable as one moves from one place to another. This variability can be caused by several factors, including (1) variations in air temperature and radiation balance, (2) local orographic influences on precipitation and storm movement, (3) the topographic variability of the ground surface, and (4) snow transport due to avalanches. However, when viewed on a small local scale (say 5 to 500 meters) these factors are generally considered secondary processes. The dominant process which

produces spatially varying snow depths is the
redistribution of snow by wind; this generally occurs
during or following precipitation or storm events.

The spatial distribution of seasonal snow is a
significant feature of both middle and upper latitude
environments. Its influence on both global and local
scales is dramatic. On the global scale, the
interaction between heat gain at low latitudes, and heat
loss at high latitudes, is the primary mechanism driving
global atmospheric circulation and weather patterns.
Since snow covered surfaces have a much higher albedo
(surface reflectivity) than vegetated surfaces, the
seasonal snow distribution in high latitudes strongly
influences the earth's radiation balance (McFadden and
Ragotzkie, 1967). As a consequence, snow distribution
is a critical parameter affecting global circulation and
climate.

On the local scale, the seasonal snow distribution
is an important hydrological parameter affecting
farmland irrigation, hydroelectric power, and water
supplies for business and domestic use. The snowcover
is also utilized as a recreation medium, providing sport
for skiers, snowmobilers, and other winter outdoor
enthusiasts. The hazardous aspect of snow affects
transportation by reducing visibility, forming drifts on

roadways, and reducing traction. In addition, hazards such as snow avalanches and snowmelt flooding may pose a threat to both property and life.

In Arctic Alaska, seasonal snow is a dominant feature of the landscape for nine months of each year. Several problems have been identified which relate directly to the spatial variation of this snowcover. In regions lacking sufficient fresh water supply due to lack of runoff or suitable reservoirs, for instance, there is an interest in accumulating snow into large drifts to serve as summer water sources (Slaughter et al., 1975). In addition, the petroleum industry spends millions of dollars annually, removing snow from materiel sites, drill pads, and roads at their arctic drilling locations. Furthermore, Federal regulations designed to protect underlying arctic vegetation stipulate, based on snowcover amount, when travel across the arctic tundra is permissible. Only through knowledge of snow distribution patterns can this determination be made accurately and thus fulfill its intended objective.

In Antarctica, a continent where more than 95 percent of the land area is covered by a blanket of snow and ice, blowing and drifting snow has been a significant factor affecting all research and

exploration conducted there. The United States
Antarctic Research Program bases McMurdo and South Pole,
for instance, continually have to deal with drifting
snow. The continent is a desert with low annual snow
accumulation, but since little of it melts, the supply
of snow for drifting is literally limitless. At McMurdo
Station, the buildings at the near-by air field are
virtually buried by drifting snow during the long winter
months. Crews spend much of the austral summer digging
these buildings out and moving the snow far enough away
so it won't induce further drifting. At South Pole
Station, where the air temperature never rises above
freezing, snow removal is a never ending task. In spite
of the crews' efforts, the station is slowly being
drifted under.

Snowcover influences not only the activities of
people, but also flora and fauna are affected by its
distribution. Vegetation growth is influenced by spring
and summer snowmelt from drifts formed the previous
winter. In addition, winter wheat crops in the northern
latitudes require the insulation provided by snowcover
to withstand low winter temperatures. The depth of snow
dictates where livestock, deer, elk, and moose can feed.
Also, microtine rodents living beneath the snow depend
on it for protection from predators and from extremes of

wind and temperature in the environment above.

Despite the significant role that snow accumulation patterns play in our lives and the world around us, severe deficiencies exist in our ability to describe and model the relevant processes and resulting snow distribution. Here I attempt to fill some of these deficiencies as well as provide a contribution to disciplines interested in describing turbulent-sediment transport.

This research project studies the blowing and drifting snow problem and develops a physically based model describing its significant features. While the current knowledge base is concerned largely with one-dimensional flows, a unique feature of this study is a focus on two-dimensional flows. The current state of understanding and technology clearly indicates the need and capability to make the next step forward and describe this more complex flow configuration. Recent advances in modeling turbulent two-phase flows provide an exciting opportunity to use this information to develop a computational model of snow transport processes.

In blowing and drifting snow, two distinct flow regimes are found. At the surface is the saltation layer. This layer is approximately 5 cm thick and is

characterized by particles repeatedly impacting the surface, dislodging additional particles into the air to be brought back to the surface under the influence of gravity. Above this layer, the flow can be described as a turbulent, two-phase mixture of air and snow particles. These two layers are highly coupled, and therefore an accurate description of the general snow transport process relies heavily on the descriptions of motions contained within both of these layers.

A model is developed which describes the turbulent air and snow mixture flowing above the saltation layer. A saltation model is then adopted and the two models are coupled through their common boundary and used to describe the fundamental features of the blowing and drifting snow problem. Features to be described include (1) the flow field of the turbulent air-snow mixture, (2) the snow concentration field within the air-snow mixture, and (3) the resulting snow accumulation profiles. Published experimental results are used to evaluate the computational model.

CHAPTER 2

PREVIOUS WORK ON BLOWING AND DRIFTING SNOW

Past studies of blowing and drifting snow can roughly be broken into two general categories: those studying the physical characteristics of the process, and those modeling the process and effects. Investigations of the physical characteristics of blowing and drifting snow have been largely observational in nature. These studies include measurements of particle size distributions, saltation parameters, flux profiles, and drift formations around natural and created obstructions to the flow.

Detailed reviews of many of these studies can be found in Mellor (1965, 1970), Radok (1977), Male (1980), Kind (1981), and Schmidt (1982a). The results of these reviews and the following cited literature is not summarized here. They are presented as an indication of the information available on this subject.

Particle size distributions have been measured by Budd (1966), Budd et al. (1966), and Schmidt (1981, 1982b, 1984). Vertical flux profiles are described by

Budd et al. (1966), Fohn (1980), Takeuchi (1980), Schmidt (1982b, 1986a), Schmidt et al. (1982), and Schmidt et al. (1984). Sublimation from blowing snow particles is discussed by Dyunin (1967), Schmidt (1972, 1982b), Tabler and Schmidt (1972), Lee (1975), Tabler (1975a), Male (1980), and Benson (1982).

Studies focusing on the saltation process include Bagnold (1941), Mellor and Radok (1960), Jenssen (1963), Owen (1964), Oura (1967), Oura et al. (1967), Kobayashi (1972, 1979), Kind (1976), White and Schluz (1977), Maeno et al. (1979), and Kind and Murray (1982). The influence of snow surface hardness on snow transport is studied by Dyunin (1963), Bagnold (1966), Narita (1978), Schmidt (1980, 1981, 1986a, 1986b), and Martinelli and Ozment (1985).

Measurement of snowdrift profiles in natural topographic catchments include those made by Berg and Caine (1975), Tabler (1975b), Benson (1982), Berg (1986), and Liston (1986). Profiles of snowdrifts formed by snow fences are described by Tabler (1980).

The preceding studies represent a world-wide effort to obtain a better understanding of the physical principles governing drifting snow and the saltation process. They are all observational.

The second classification of the drifting snow

studies encompasses those which model the drifting process and/or effects. The complexity of the factors influencing snowdrift patterns formed by structures and terrain features has lead to the simulation of blowing snow and drift formations using wind tunnels and water flumes. Finney (1934) introduced this technique using sawdust and mica in a wind tunnel. In order to assure quantitative scaling of the snowdrifts, certain theoretical requirements must be met. However, these requirements cannot be entirely realized, and consequently compromises must be made if this approach is used (Iversen, 1979, 1980; Anno, 1984a; Kind, 1986). Reduced-scale model experiments, performed outside in natural conditions instead of within a wind tunnel, have been used in an attempt to avoid these restrictive scaling requirements (Tabler and Jairell, 1981; Anno, 1984b).

Empirical models have also been produced. Tabler (1975b) developed a multiple linear regression equation which predicts equilibrium profiles of snowdrifts in topographic catchments. This type of model is generally considered appropriate only for the conditions under which the regression coefficients were originally determined. Similarly, Tabler (1980) developed polynomial regression curves which describe equilibrium

snowdrift profiles produced by snow fences.

A computer simulation model which predicts the accumulation of wind-blown snow particles in topographic catchments is presented by Berg and Caine (1975) and Berg (1986). The model comprises a set of mathematical relationships between airflow, topography, and snow particle movement that determine regions where the windspeed is below the threshold required for snow transport and then consequently accumulates particles in such regions.

Recently, computational and physical modeling efforts have been implemented in an attempt to (1) explain the physical processes associated with snow transport and (2) develop predictive tools for these processes. Decker and Brown (1983, 1985) utilized modern mixture theory to study blowing snow in mountainous terrain. This study was aimed at predicting snow deposition patterns in mountainous terrain and determining the nature of the dominant processes governing two phase flow of air and suspended snow particles. Uematsu et al. (1989) developed a two-dimensional finite element model of snowdrift development. They solve the momentum equations assuming a constant eddy or turbulent diffusivity.

The picture that emerges from this review is that

the vast majority of previous snow transport studies
have been observational in nature, and very little
computational modeling of the relevant flow features and
processes has been attempted.

CHAPTER 3

MATHEMATICAL MODEL DEVELOPMENT

In this chapter the governing equations and turbulence modeling practices for both single-phase and two-phase flows are presented. The governing equations of fluid motion represent a description of the time and spatial variation of velocity and pressure for the flow of concern. In engineering and atmospheric sciences the flows of interest are almost always turbulent. A turbulent flow is characterized by fluid motion which is eddying, highly random, unsteady, and three-dimensional. These eddies cover a wide spectrum of sizes, ranging from the size of the flow domain to many orders of magnitude smaller, and they also cover a correspondingly wide range of fluctuation frequencies with the high frequencies being associated with the small eddies. Commonly the turbulent fluctuations are removed from the flow description by a suitable averaging of the governing equations. This averaging leads to new terms which contain unknown correlations between fluctuating velocity components. A non-closed system of equations

results since the number of unknown variables now exceeds the number of equations. To close the system of equations a turbulence model must be developed which relates the new unknown quantities to the mean flow field.

Turbulence Modeling for Single-Phase Flows

The governing equations of fluid motion are based on the universal conservation laws of mass and momentum. The resulting continuity and momentum equations for a Newtonian fluid are commonly referred to as the Navier-Stokes equations and take the following form for an incompressible fluid (Schlichting, 1979),

Continuity Equation:

$$\frac{\partial U_i}{\partial x_i} = 0 \tag{1}$$

Momentum Equations:

$$\frac{\partial U_i}{\partial t} + U_j \frac{\partial U_i}{\partial x_j} = -\frac{1}{\rho} \frac{\partial P}{\partial x_i} + \nu \frac{\partial^2 U_i}{\partial x_j \partial x_j} \tag{2}$$

where U_i is the instantaneous velocity component in the x_i direction, t is time, P is pressure, ρ is the fluid density, and ν is the kinematic viscosity. Here the Einstein summation convention on repeated indices has been applied.

The unsteady Navier-Stokes equations are generally considered to be capable of describing turbulent flow. Direct simulation of the turbulent flow is impractical, however, because the scale of the smallest eddies in turbulent flow is typically 10^{-3} times the size of the flow domain. A common estimation is that a numerical grid containing 10^5 points would be required to resolve just 1 cm^3 of the flow. As a consequence, it is not expected that computers will be large and fast enough to describe the flow field in this manner in the near future.

The common approach used today is to solve for the mean flow field using the equations which have been averaged over a time which is long compared with the turbulence but short when compared to that of the mean flow. In this approach, the instantaneous values of velocity U_i and the pressure P are separated into mean (overbars) and fluctuating (lower case) quantities

$$U_i = \overline{U_i} + u_i \quad , \quad P = \overline{P} + p \tag{3}$$

and the mean quantities are given by

$$\overline{U_i} = \frac{1}{t_2 - t_1} \int_{t_1}^{t_2} U_i \, dt \quad , \quad \overline{P} = \frac{1}{t_2 - t_1} \int_{t_1}^{t_2} P \, dt \tag{4}$$

Carrying out the averaging procedure leads to the following equations, where the overbars have been dropped for efficiency, except where averages of products of fluctuating terms are needed for clarity.

Continuity Equation:

$$\frac{\partial U_i}{\partial x_i} = 0 \tag{5}$$

Momentum Equations:

$$\frac{\partial U_i}{\partial t} + U_j \frac{\partial U_i}{\partial x_j} = - \frac{1}{\rho} \frac{\partial P}{\partial x_i} + \frac{\partial}{\partial x_j}\left(\nu \frac{\partial U_i}{\partial x_j} - \overline{u_i u_j}\right) \tag{6}$$

These time averaged Navier-Stokes equations are often called the Reynolds averaged equations after their original developer, Osborne Reynolds, and they govern the mean flow quantities U_i and P. The time averaging has led to new terms $\overline{u_i u_j}$, in the momentum equations which, when multiplied by ρ, are interpreted as stresses associated with the turbulent motion. These turbulent stress components are frequently many orders of magnitude larger than the viscous stresses found in the term containing ν. These new terms must now be modeled or described in terms of the mean flow variables in order to create a closed set of equations.

Existing turbulence models which approximate these

terms range from simple models based on Prandtl's mixing-length hypothesis (Schlichting, 1979) to those that use differential transport equations for the individual turbulent stresses and fluxes. Extensive reviews of the various models can be found in Rodi (1982) and Lakshminarayana (1986).

The simple models based on the Prandtl mixing-length hypothesis suffer from several drawbacks. One primary failing is that the hypothesis implies that the turbulence is in local equilibrium, consequently the model is unable to account for the transport and history effects of turbulence. This leads to incorrectly predicting zero turbulence in flow regions of uniform mean velocity where the velocity gradient is zero. Examples of this problem include the prediction of zero turbulence in both the center of a pipe and in the flow behind a uniform grid (Rodi, 1980). It is also worth noting that since it is difficult to prescribe the mixing-length distribution in any but the simplest flows, these models are not applicable to more complex, separating flows.

Efforts to develop a more universal turbulence model has led to what is known as the k-ϵ model of Jones and Launder (1972). This is a two-equation model which uses two partial differential transport equations to

describe evolution of the turbulent kinetic energy k, and the dissipation rate ϵ, of the turbulent kinetic energy. The turbulent kinetic energy k, where k is defined to be

$$k = \frac{1}{2} \overline{u_i u_i} = \frac{1}{2} \left(\overline{u_1^2} + \overline{u_2^2} + \overline{u_3^2} \right) \tag{7}$$

and a length scale L, which describes the characteristic size of large eddies producing turbulent stresses, are frequently viewed as the primary parameters which allow description of turbulent flows. Since the rate of dissipation ϵ is proportional to $k^{3/2}/L$ (Rodi, 1980), a description of the variation of k and ϵ will allow an indirect description of the characteristic turbulent length scale.

In laminar flows the viscous stresses are proportional to the mean velocity gradients; with the kinematic viscosity ν of the fluid serving as the proportionality constant. To develop the k-ϵ model the turbulent stresses $\overline{u_i u_j}$ are first assumed to be related to the mean velocity gradients by Boussinesq's eddy viscosity hypothesis

$$- \overline{u_i u_j} = \nu_t \left(\frac{\partial U_i}{\partial x_j} + \frac{\partial U_j}{\partial x_i} \right) - \frac{2}{3} k \delta_{ij} \tag{8}$$

where ν_t is the turbulent viscosity and δ_{ij} is the Kronecker Delta function. Here the turbulent viscosity ν_t is a property of the flow rather than the fluid, and it may vary greatly over the flow field. Equation 8 contains two new unknowns ν_t and the turbulent kinetic energy k. Since it is difficult to derive an expression directly for ν_t, it was reasoned, by dimensional analysis, that ν_t is proportional to k^2/ϵ where ϵ is the dissipation rate of k (Jones and Launder, 1972). Thus it is assumed that

$$\nu_t = C_\mu \frac{k^2}{\epsilon} \qquad (9)$$

where C_μ is a constant. At this stage the problem has been shifted from describing the Reynolds stresses, to describing the distribution of k and ϵ.

An exact equation for the Reynolds stresses $\overline{u_i u_j}$ can be derived from the Navier-Stokes equations. To do this, the time averaged momentum equations (Equation 6) are subtracted from the time dependent Navier-Stokes equations (Equation 2) for both velocity components i and j. The equation for u_i is then multiplied by u_j and the equation for u_j by u_i, and the two resulting equations are added. Time averaging this last equation, and assuming the viscous diffusion term is negligible in

high Reynolds number flows, yields (Hinze, 1975),

$$\frac{\partial \overline{u_i u_j}}{\partial t} + U_l \frac{\partial \overline{u_i u_j}}{\partial x_l} = -\frac{\partial}{\partial x_l}\left(\overline{u_l u_i u_j}\right) - \frac{1}{\rho}\left(\frac{\partial \overline{u_j p}}{\partial x_i} + \frac{\partial \overline{u_i p}}{\partial x_j}\right)$$

$$- \overline{u_i u_l}\frac{\partial U_j}{\partial x_l} - \overline{u_j u_l}\frac{\partial U_i}{\partial x_l} + \overline{\frac{p}{\rho}\left(\frac{\partial u_i}{\partial x_j} + \frac{\partial u_j}{\partial x_i}\right)} - 2\nu\overline{\frac{\partial u_i}{\partial x_l}\frac{\partial u_j}{\partial x_l}}$$

(10)

When these three equations for the three normal stresses (i=j=1,2,3) are summed, an exact equation for the turbulent kinetic energy is obtained (Rodi, 1984),

$$\frac{\partial k}{\partial t} + U_i\frac{\partial k}{\partial x_i} = -\frac{\partial}{\partial x_i}\left(\overline{u_i\left(\frac{u_j u_j}{2} + \frac{p}{\rho}\right)}\right) - \overline{u_i u_j}\frac{\partial U_i}{\partial x_j}$$

$$- \nu\overline{\frac{\partial u_i}{\partial x_j}\frac{\partial u_i}{\partial x_j}}$$

(11)

In this equation the rate of change of k is balanced by convective transport due to the mean flow, diffusive transport due to velocity and pressure fluctuations, production of turbulent kinetic energy due to the combination of Reynolds stresses and mean velocity gradients, and dissipation of k by the transfer of kinetic energy into heat.

For this k equation to be applied to the momentum equations, the additional unknown terms in this equation must be modeled. Applying the Boussinesq eddy viscosity hypothesis, the term describing the production of k due

to the interaction of Reynolds stresses and velocity
shear becomes

$$- \overline{u_i u_j} \frac{\partial U_i}{\partial x_j} = \nu_t \left(\frac{\partial U_i}{\partial x_j} + \frac{\partial U_j}{\partial x_i} \right) \frac{\partial U_i}{\partial x_j} \tag{12}$$

The diffusive transport term is modeled as

$$- \left(\overline{u_i \left(\frac{u_j u_j}{2} + \frac{p}{\rho} \right)} \right) = \frac{\nu_t}{\sigma_k} \frac{\partial k}{\partial x_i} \tag{13}$$

where σ_k is a constant. The last term describes the
product of the molecular kinematic viscosity and the
fluctuating vorticity, or the rate of viscous
dissipation of energy ϵ,

$$\nu \overline{\frac{\partial u_i}{\partial x_j} \frac{\partial u_i}{\partial x_j}} = \epsilon \tag{14}$$

The final, most common form of the turbulent
kinetic energy transport equation is

$$\frac{\partial k}{\partial t} + U_i \frac{\partial k}{\partial x_i} = \frac{\partial}{\partial x_i} \left(\frac{\nu_t}{\sigma_k} \frac{\partial k}{\partial x_i} \right) + \nu_t \left(\frac{\partial U_i}{\partial x_j} + \frac{\partial U_j}{\partial x_i} \right) \frac{\partial U_i}{\partial x_j} - \epsilon \tag{15}$$

$$\text{(i)} \quad \text{(ii)} \quad \text{(iii)} \quad \text{(iv)} \quad \text{(v)}$$

where term (i) represents the rate of change of k, term
(ii) describes convective transport of k, term (iii) is
the diffusive transport, term (iv) describes the

production of k through shear, and term (v) is the rate of viscous dissipation.

An exact transport equation for ϵ can also be derived from the Navier-Stokes equations for high Reynolds number flows (Hanjalic and Launder, 1972),

$$\frac{\partial \epsilon}{\partial t} + U_i \frac{\partial \epsilon}{\partial x_i} = -2\nu\left(\overline{\frac{\partial u_j}{\partial x_l}\frac{\partial u_i}{\partial x_l}} + \overline{\frac{\partial u_l}{\partial x_i}\frac{\partial u_l}{\partial x_j}}\right)\frac{\partial U_i}{\partial x_j}$$

$$-2\nu\overline{\frac{\partial u_j}{\partial x_l}\frac{\partial u_i}{\partial x_l}\frac{\partial u_j}{\partial x_i}} - 2\nu^2\overline{\left(\frac{\partial^2 u_j}{\partial x_i \partial x_l}\right)^2} - \frac{\partial}{\partial x_i}\overline{u_i \epsilon'} \tag{16}$$

where ϵ' describes the fluctuating dissipation rate. Again there have been new terms introduced which must be modeled in order to obtain a closed set of equations (Hanjalic and Launder, 1972). The first term on the right is a generation term which is modeled as

$$-2\nu\left(\overline{\frac{\partial u_j}{\partial x_l}\frac{\partial u_i}{\partial x_l}} + \overline{\frac{\partial u_l}{\partial x_i}\frac{\partial u_l}{\partial x_j}}\right) = C_{1\epsilon}\epsilon\frac{\nu_t}{k}\left(\frac{\partial U_i}{\partial x_j} + \frac{\partial U_j}{\partial x_i}\right) \tag{17}$$

where $c_{1\epsilon}$ is a modeling constant. The second and third terms are modeled together in the form

$$2\nu\overline{\frac{\partial u_j}{\partial x_l}\frac{\partial u_i}{\partial x_l}\frac{\partial u_j}{\partial x_i}} + 2\nu^2\overline{\left(\frac{\partial^2 u_j}{\partial x_i \partial x_l}\right)^2} = C_{2\epsilon}\frac{\epsilon^2}{k} \tag{18}$$

where $c_{2\epsilon}$ is a constant. The fourth term describes the diffusion of ϵ due to velocity fluctuations and becomes

$$- \overline{u_i \epsilon'} - \frac{\nu_t}{\sigma_e} \frac{\partial \epsilon}{\partial x_i} \qquad (19)$$

where σ_ϵ is a constant. The most common form of the modeled ϵ equation is

$$\frac{\partial \epsilon}{\partial t} + U_i \frac{\partial \epsilon}{\partial x_i} - \frac{\partial}{\partial x_i}\left(\frac{\nu_t}{\sigma_e} \frac{\partial \epsilon}{\partial x_i} \right)$$

$$+ C_{1\epsilon} \epsilon \frac{\nu_t}{k}\left(\frac{\partial U_i}{\partial x_j} + \frac{\partial U_j}{\partial x_i} \right) \frac{\partial U_i}{\partial x_j} - C_{2\epsilon} \frac{\epsilon^2}{k} \qquad (20)$$

where each term has a meaning similar to those found in the k equation.

In engineering applications the empirical constants most frequently used in these equations are: $C_\mu = 0.09$, $C_{1\epsilon} = 1.44$, $C_{2\epsilon} = 1.92$, $\sigma_k = 1.0$, $\sigma_\epsilon = 1.3$ (Launder and Spalding, 1974). These constants have been found to successfully predict mean flow characteristics for a large variety of flows including flows having a free surface and those involving recirculation. Over the past 15 years the k-ϵ model has been tested extensively and has found success for a variety of different flows, including free shear flows, wall boundary layers, flows involving recirculation, and duct flows (Rodi, 1982).

Hanjalic and Launder (1980) proposed that an

additional term be added to increase the rate of
irrotational deformations in promoting turbulent energy
transfer. Rodi (1985) developed a buoyancy-extended k-ϵ
model which is used to model horizontal shear layers
with stable stratification. This paper is essentially a
simplification of the transport equation model of Gibson
and Launder (1978).

A further step in turbulence model complexity is
the second-order closure schemes which employ transport
equations to describe the individual stresses and
fluxes. This eliminates the assumption of local
isotropy found in the k-ϵ model. Although these models
contain fewer assumptions and are much more general than
the simpler models, they also contain additional terms
which must be modeled based on approximations and
assumptions of flow properties, some of which are still
unable to be measured. In addition, the large number of
partial differential equations involved make these
models computationally cumbersome. At this stage, these
very complex models are considered to be subjects of
turbulence research and are not sufficiently refined for
application to practical problems. The stress and flux
transport equations can be reduced, however, to
algebraic equations which still maintain many of the
important characteristics of the more complex equations.

These algebraic equations are then combined with the k
and ε equations to simulate the turbulent stresses
(Lakshminarayana, 1986).

A completely different approach is called large
eddy simulation. In this scheme the large scale
turbulence, which is responsible for the majority of the
flow behavior, is simulated numerically while a model is
used to describe the small scale turbulence structure
(Peyret and Taylor, 1983). This computationally tedious
method also shows much promise but is still largely in
its developmental stages.

Turbulence Modeling for Two-Phase Flows

As early as 1945 research showed that adding a
dilute suspension of particles to a turbulent fluid
increases the flow rate under a given pressure gradient
(Sproull, 1961). Hetsroni and Sokolov (1971) concluded
that the particles suppress the turbulence in the
dissipation range of small eddies and that the process
is dependent upon both particle size and concentration.
Moderrass et al. (1984) showed that, depending on
particle loading, the turbulent kinetic energy can be
reduced as much as 50 percent, thereby increasing the
carrier fluid velocity. This process is again
attributed to a decrease in turbulence dissipation

resulting from particle-fluid interaction.

Two common approaches are taken to describe fluid-particle flows, the trajectory approach and the two-fluid approach. In the trajectory approach the turbulent flow field is first calculated assuming single phase flow. Then particle velocities and trajectories are calculated using the single-phase flow field. A major shortcoming of this is the assumption that the presence of particles does not influence the motion of the fluid. This results in what is known as a one-way coupling of the phases. This method can be extended by recalculating the flow field with the inclusion of the calculated particle behavior. The particle trajectories are again calculated based on the flow field and this process is repeated until the flow field does not change with subsequent iterations. In this manner the trajectory approach is able to include the two-way coupling which commonly characterizes two-phase flows (Crowe, 1982). Two-way coupling is also included when using the two-fluid approach. This approach regards the fluid and particulate phases as two interacting fluids which are governed by their own mass balance and momentum balance equations.

In this study the author will consider only dilute particle suspensions where the particulate phase volume

fraction is small (of order 10^{-3}), and particle to
particle interactions can be considered negligible. For
this case, the governing equations of motion can be
described as taking the same form as the previously
introduced Navier-Stokes and Reynolds averaged
equations, where an additional source term F_p has been
added to the right side of the momentum equations to
account for the force exerted upon the fluid by the
particles (Marble, 1970).

Two-phase turbulence closure modeling is a
relatively new field of study. Danon et al. (1977)
proposed a one-equation, one-way coupled model for a
very lightly loaded flow. Melville and Bray (1979)
produced an algebraic model based on the Prandtl mixing-
length hypothesis for moderately loaded jets. Genchev
and Karpunov (1980) developed a mixing-length model
which includes an extra term which takes into account
the particle influence on turbulent motion. Their
results are not compared to experimental data.
Elghobashi and Abou-Arab (1983) presented a complex,
two-equation closure scheme for two-phase flows which
attempts to resolve some of the weaknesses of the
schemes of Danon et al. and Genchev and Karpunov.
Decker and Brown (1985) modeled the turbulent
fluctuations of the particulate phase based on the

mixing-length hypothesis and applied it to a one-way coupled mixture of air and snow.

One of the most advanced and extensively tested modeling efforts has been that of Chen (1983) and Chen and Wood (1984; 1985). It is assumed that the particulate phase volume fraction is much less than unity and made up of spherical particles of uniform size.

Their model is based on the two-equation k-ϵ turbulence model described previously. Here an additional term, which results from including a particle-fluid interaction force, is added to each of the k and ϵ turbulence equations. It is assumed that the particles follow the mean flow, but that on the high frequency turbulent fluctuation level, the particles do not exactly follow the fluid and the resulting slip is a hydrodynamic drag force F_p which can be described by Stokes law and takes the form,

$$F_p = \frac{\rho_p (V_i - U_i)}{t^*} \qquad (21)$$

where U_i and V_i represent the fluid and particle velocities, respectively. ρ_p is the particulate phase density, and $t^* = d^2 \rho_s / 18\mu$ is the characteristic response time of the particles; d is the particle diameter, ρ_s is

the density of the solid particulate material, and μ is the fluid viscosity. This approach appears to be valid for the dilute mixture considered here. Experimental data by Popper et al. (1974) and Yuu et al. (1978) suggest that, to a first approximation, we can assume that the particles follow the mean motion but not necessarily the turbulent fluctuations.

A derivation of the turbulence kinetic energy equation with the inclusion of the Stokes drag force in the momentum equations produces an additional term in the k equation which takes the form (Chen and Wood, 1984),

$$\frac{\rho_p}{\rho} \frac{\left(\overline{u_i v_i - u_i u_i}\right)}{t^*} \qquad (22)$$

where v_i is the fluctuating particulate velocity. This new term represents additional dissipation resulting from particle slip at the turbulent fluctuation level. This term is modeled by letting

$$- \left(\overline{u_i v_i - u_i u_i}\right) - 2 k \left(1 - \exp\left(-B_k \frac{t^*}{t_e}\right)\right) \qquad (23)$$

where $t_e = 0.165 \, k/\epsilon$, and B_k is a constant set equal to 0.0825 (Chen and Wood, 1985).

The dissipation rate equation for ϵ will also have an additional term

$$\frac{2}{t^*} \frac{\rho_p}{\rho} \left(\nu \overline{\frac{\partial u_i}{\partial x_j} \left(\frac{\partial v_i}{\partial x_j} - \frac{\partial u_i}{\partial x_j} \right)} \right) \qquad (24)$$

which is modeled as

$$- \left(\nu \overline{\frac{\partial u_i}{\partial x_j} \left(\frac{\partial v_i}{\partial x_j} - \frac{\partial u_i}{\partial x_j} \right)} \right) - \epsilon \left(1 - \exp \left(-B_\epsilon \frac{t^*}{\tau} \right) \right) \qquad (25)$$

where $\tau = (\nu/\epsilon)^{1/2}$ is the Kolmogorov time scale frequently used to describe high frequency eddies and B_ϵ is a modeling constant.

These modeled terms, when added to the right side of the appropriate k and ϵ equations, produce additional dissipation which reduce turbulent velocity fluctuations.

Since the two additional particulate terms depend on the dimensionless particulate phase loading ρ_p/ρ, an additional transport equation must be solved to determine the particle concentration field. This equation accounts for particulate mass conservation and takes the following form (Rodi, 1984),

$$\frac{\partial w}{\partial t} + U_i \frac{\partial w}{\partial x_i} - \frac{\partial}{\partial x_i} \left(\frac{\nu_t}{\sigma_t} \frac{\partial w}{\partial x_i} \right) \qquad (26)$$

where the particulate concentration $w = \rho_p/\rho$, and σ_t is
the turbulent Schmidt number = 0.5 for planar flows
(Reynolds, 1976).

Saltation Modeling

Saltation is a process in which snow particles are
transported close to the ground, undergoing repeated
impacts with the snow covered surface. Initially loose
snow particles are entrained into the air stream by the
wind. After having gained momentum from the wind they
fall back to the ground to strike other snow particles
on the snow covered surface. Most of the time the
impacting particle rebounds from the surface and is
accelerated by the wind before it again falls to the
ground. Since the impact with the surface is inelastic,
the rebound velocity is necessarily less than the impact
velocity. Since the surface is rough, on a scale
comparable to the particle size, the impacting particle
rebounds at an angle different than the impact angle.
In order to sustain saltation, the average vertical
rebound velocity must equal the incident vertical
velocity. If it is less, the vertical velocity will die
out after several impacts and the particle will cease to
saltate. During impact a particle may also dislodge
additional snow particles from the snow surface. While

some of these particles may then join the saltation process, others may roll or bounce over short distances to form a layer of reptating particles. As more particles are added to the airstream, the speed of the wind in the saltating layer is reduced. This reduces the impact velocity of the saltating particles which in turn decreases the average vertical rebound velocity. In addition, as the impact velocity decreases, the effectiveness of an impacting particle at ejecting more particles into the flow decreases. Thus, snow particles begin to settle out of the saltating layer. As the particles start to settle out, the wind deceleration is reversed, allowing more particles to be entrained. An equilibrium is eventually reached for a given free stream airflow, and only a certain number of particles are maintained in the saltating layer.

Measurements above a horizontal surface show a very rapid decrease in mass flux with height through the saltation layer. In fact, Kind (1981), using data provided by Oura (1967) and Kobayashi (1972), reported that approximately 90 percent of the total saltating mass flux is contained within the first 3 cm above the surface.

The presence of saltation is dependent upon the relative magnitudes of the shear strength of the snow

surface and the shear stress at the surface produced by the wind above. In order for snow particles to begin to move, some threshold shear stress must be exceeded. This threshold value is dependent upon such factors as temperature, grain size, extent of grain bonding, and surface hardness. Kind (1981) lists experimental studies which have found threshold shear velocity values ranging from 0.1 m/s for light dry snow, to 0.4 m/s for old hardened snow.

One saltation model which has found considerable favor in the literature was developed by Iversen et al. (1975) based on similitude arguments. Schmidt (1982a) has shown this model to successfully reproduce field data collected by several researchers. The model takes the form

$$Q_s = C\left(\frac{\rho}{g}\right)\left(\frac{V_s}{U_{*t}}\right) U_*^2 (U_* - U_{*t})\qquad(27)$$

where Q_s is the total mass transport rate per unit lateral dimension with units of kg/(m s), ρ is the fluid density, g is the gravitational acceleration, V_s is the settling velocity of a snow particle, U_* is the friction or shear velocity, U_{*t} is the threshold shear velocity, and C is a constant set equal to 1.0.

Since the majority of the mass flux is confined to

the area very near the ground, and a computation of the turbulent flow field above the surface will provide values of the surface shear velocity, the computed upper flow field will be used to drive the saltation model. Here the turbulent layer's sole purpose is to drive the saltation model which is responsible for the greatest contribution of snow transport.

As presented, the coupling between the turbulent and saltation layers has been assumed passive or one-way, i.e., the presence or lack of saltation does not affect the solution of the turbulent flow field. Initially, it appears that the two-way coupling which occurs in the natural system is only a secondary process. Consequently, the one-way coupling approximation will be assumed valid.

The saltation model provides the vertically integrated rate of snow transport, $Q_s(x)$, within that layer. Knowledge of the particulate concentration and velocity fields allow computation of the vertically integrated rate of snow transport within the turbulent flow layer, $Q_t(x)$, where

$$Q_t(x) - \int U(x,z) \ w(x,z) \ dz \qquad (28)$$

Changes in the bed surface level (snow accumulation
or drift formation) result from changes in Q_t and Q_s
with x. This change in surface level is described by
the vertically integrated mass continuity equation,

$$\frac{\partial h}{\partial t} + \frac{1}{\rho_b} \frac{\partial}{\partial x} (Q_t + Q_s) = 0 \qquad (29)$$

where h is the surface level with respect to a
horizontal datum, t = time, and ρ_b is the bulk density
of snow. The accumulation of mass, and subsequent new
boundary configuration, necessitates a recomputation of
the turbulent flow field.

CHAPTER 4

TWO-PHASE TURBULENT FLOW MODEL FOR BLOWING SNOW

Governing Equations

In the previous chapter the ground work was set for developing a model for application to blowing and drifting snow. As a rigorous test case for the model the flow over a two-dimensional obstruction, such as an infinitely long solid wall 2 meters high and aligned perpendicular to the wind direction, will be considered (Figure 1). Developing the governing equations for this problem will begin with the Reynolds averaged equations. Since the flow of interest will contain significant zones of recirculation, boundary layer approximations will not apply and the Reynolds equations must be solved in their full form. In addition to the two-dimensional restriction, only steady state flows will be considered. As such, the previously introduced Reynolds equations and the k and ϵ turbulence model equations will apply with the neglect of the appropriate terms. Also, as noted previously, since the kinematic viscosity ν is
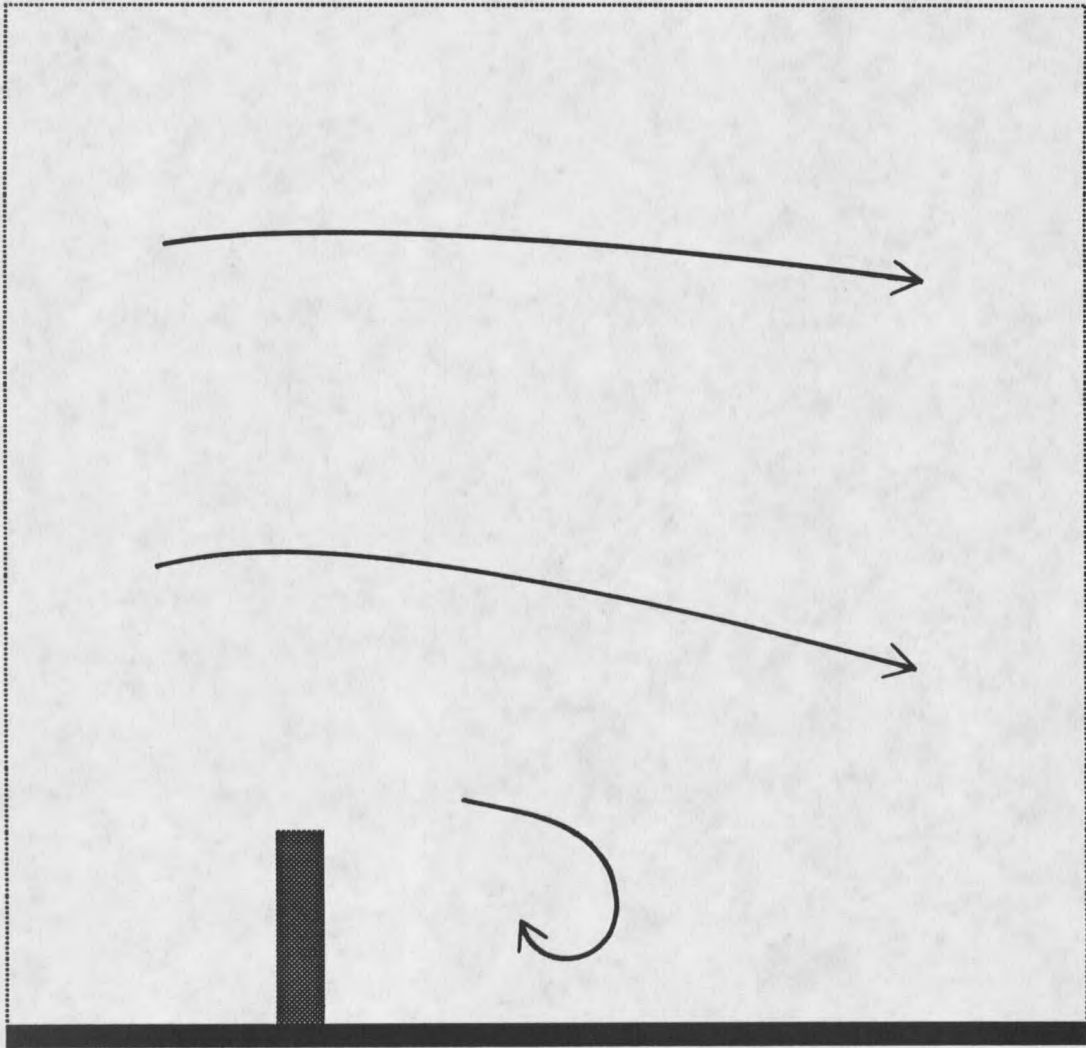
Figure 1. Computational domain boundary configuration.

typically several orders of magnitude smaller than the turbulent viscosity ν_t, the term containing ν in the time averaged momentum equations (Equation 6), will be neglected.

To establish the exact form that the momentum equations will take, Equation 8 must be introduced into Equation 6 to eliminate the $\overline{u_i u_j}$ term. When doing this it is noted that the Kronecker Delta term in Equation 8 is a pressure-like term which can be absorbed into the momentum equation pressure term. The diffusion terms in the momentum equations now take the form

$$\frac{\partial}{\partial x_j}\left(\nu_t\left(\frac{\partial U_i}{\partial x_j} + \frac{\partial U_j}{\partial x_i}\right)\right) \tag{30}$$

This can be expanded for the dimensions x and z, respectively, in the horizontal and vertical directions. By applying the continuity equation (Equation 5) and the property that in a discrete difference scheme products are interchangeable, the term becomes

$$\frac{\partial}{\partial x}\left(\nu_t\frac{\partial U}{\partial x}\right) + \frac{\partial}{\partial z}\left(\nu_t\frac{\partial U}{\partial z}\right) \tag{31}$$

for the x momentum equation with velocity U. A similar
term is found for the z momentum equation with velocity
V. Combining this information and expanding the other
indexed terms in the continuity equation and momentum
equations leads to three of the equations comprising the
turbulent flow model. They will be listed with the
other equations at the end of this chapter.

The k and ϵ equations include a production term,
resulting from shear, of the form

$$\left(\frac{\partial U_i}{\partial x_j} + \frac{\partial U_j}{\partial x_i}\right) \frac{\partial U_i}{\partial x_j} \tag{32}$$

When this is expanded in a manner similar to the term in
the momentum equation, this term becomes

$$\left(\frac{\partial U}{\partial z} - \frac{\partial V}{\partial x}\right)^2 \tag{33}$$

Together the k and ϵ equations contain five
modeling constants, c_μ, $c_{1\epsilon}$, $c_{2\epsilon}$, σ_k, and σ_ϵ which must be
determined before the equations can be solved (Launder
and Spalding, 1974). Values for these constants were
listed in the previous chapter. How the constants were
obtained is discussed by Rodi (1984). The value of $c_{2\epsilon}$
was computed based on measurements of the decay rate of
k behind grids. Values for the diffusion constants σ_k
and σ_ϵ were obtained by a computer optimization

procedure which involved applying the model to several laboratory shear flows and adjusting the constants to achieve the best overall fit with experimental results. The final two constants, c_μ and $c_{1\epsilon}$, are evaluated by considering local equilibrium shear layers occurring near a wall. For atmospheric flows, as opposed to engineering or hydraulic flows, the values of $c_\mu = 0.03$ and $c_{1\epsilon} = 1.16$ have been suggested in the literature (Sutton et al., 1986). Since these constants agree well with atmospheric measurements (Lumley and Panofsky, 1964; Frost et al., 1975), I will adopt these atmospheric values.

The exact form of the particulate source terms in the k and ϵ equations must also be determined. To do this, representative atmospheric profiles of velocity, turbulent kinetic energy, and dissipation rate must be established.

A wide range of experimental and theoretical studies have shown that wind profiles within a surface layer of nearly hydrostatically neutral stratification can be closely approximated by a logarithmic equation. This is commonly expressed in the form (Holton, 1979),

$$U = \frac{U_*}{\kappa} \ln\left(\frac{z}{z_0}\right) \qquad (34)$$

where U_* is the shear velocity, z is the height above the surface, z_0 is the roughness length which is dependent upon the roughness of the surface, and $\kappa = 0.4$ is von Karman's constant. A roughness length of $z_0 = 0.1$ cm will be used as a representative value for snow surfaces (Sorbjan, 1989).

In a homogeneous, neutrally stratified boundary layer the rate of dissipation above the viscous sublayer is given by

$$\epsilon = \frac{U_*^3}{\kappa z} \qquad (35)$$

(Panofsky and Dutton, 1984; Sorbjan, 1989). This is also consistent with experimental data (Wyngaard and Cote, 1971). Frost et al. (1975) provided atmospheric profiles of turbulent kinetic energy k for the same conditions,

$$k = \frac{U_*^2}{\sqrt{c_\mu}} \qquad (36)$$

This agrees with field measurements by Lumley and Panofsky (1964). These profiles of U, k, and ϵ given by Equations 34, 35, and 36 can all be computed upon choosing an appropriate value for U at a specified height z. For reference, in mid-latitude regions, typical windspeeds experienced during snow transport

events fall in the range 10 to 15 m/s measured at a
height of 10 m (Kind, 1981).

The form that the particulate source terms in the k
and ϵ equations take is strongly dependent upon the
relative magnitudes of time scales t^*, t_e, and τ. To
compute t^* for a spherical ice grain in air, note that
$\rho_s = 910$ kg/m^3, $\nu = 13.3e-6$ m^2/s, and $\rho = 1.29$ kg/m^3 for
a pressure of one atmosphere and temperature of 0° C.
Applying a typical wind velocity of 10 m/s at 10 m, and
computing the values of these time scales shows that for
snow particles having diameters d ≥ 0.5 mm, $t^* \gg \tau$.
This analysis also shows that t^* and t_e are of the same
order of magnitude for this particle size range, and
that only when d ≤ 0.1 mm is $t^* \ll t_e$. The implication
of these results is that, for this study, a restriction
of d ≥ 0.5 mm allows the neglecting of the exponential
term in the ϵ equation particulate source term (Equation
25), while the k equation particulate source term
(Equation 23) must be used in its full form.

The particle concentration equation (Equation 26)
is valid as stated with the exception that a constant
particle settling velocity V_s will be added to the
vertical convection term. Here the author has assumed
that the particle concentration field is convected
downward at a velocity additional to the vertical

velocity of the fluid. A survey of published data suggests that $V_s = 0.75$ m/s is a representative still air fall velocity for snow particles of interest in this study (Mellor, 1965; Kind, 1981; Schmidt, 1982a).

Boundary Conditions

To solve the governing equations, boundary conditions must be applied at all boundaries of the computational domain for all the dependent variables. For this problem conditions U, V, P, k, ϵ, and w must all be specified in some form. A representative flow domain is depicted in Figure 1. The flow domain contains an unrestricted inflow, outflow, and top boundary as well as a solid lower boundary composed of horizontal surfaces and vertical walls. The appropriate boundary conditions are defined as follows.

Inflow boundary:

$V = 0$

U is given by Equation 34

$\dfrac{\partial(\ )}{\partial n} = 0$ for P

k is given by Equation 36

ϵ is given by Equation 35

w is set equal to a constant, $0 \le w \le 1.0$

Upper boundary:

$$\frac{\partial(\ )}{\partial n} = 0 \text{ for U, V, P, k, and } \epsilon$$

w is set equal to a constant, $0 \leq w \leq 1.0$

Outflow boundary:

$$\frac{\partial(\ )}{\partial n} = 0 \text{ for U, V, P, k, } \epsilon, \text{ and w}$$

Horizontal surfaces:

U = logarithmic

V = 0

k and ϵ are functions of the surface shear

stress through the friction velocity U_*

$$\frac{\partial(\ )}{\partial n} = 0 \text{ for P and w}$$

Vertical surfaces:

U = 0

V = 0

$$\frac{\partial(\ )}{\partial n} = 0 \text{ for P, k, and } \epsilon$$

w = 0

where n is the direction perpendicular to the boundary.

The horizontal and vertical surface type boundary conditions warrant additional discussion. The pressure boundary condition will be discussed in Chapter 5. In

developing the turbulence equations, the laminar flow within the viscous sublayer near a wall has been neglected. Turbulence models have been developed which account for these effects, but since the gradients encountered in the near-wall region are typically very steep, and consequently computationally expensive to resolve, these models are not commonly used. A far more common scheme is to choose a computational domain which is slightly removed from the solid boundary and apply semi-empirical wall functions to the gap between the solid boundary and computational boundary.

The logarithmic profile given by Equation 34 is used in this study for the U velocity boundary condition on all horizontal surfaces including the top of the wall. U is set to zero on vertical walls. The V component of velocity, which is perpendicular to horizontal surfaces, is set equal to zero, and considered negligibly small on vertical surfaces. To apply the log-wall boundary condition, a profile given by Equation 34 is assumed to exist between the solid surface at $z = 0.0$, a grid point on the computational domain boundary at $z = z_1$, and the first interior grid point at $z = z_2$. The resulting two equations for U_1 and U_2 can be equated through their common U_* and solved to yield a boundary condition of the form

$$U_1 = \frac{\ln\left(\dfrac{z_1}{z_0}\right)}{\ln\left(\dfrac{z_2}{z_0}\right)} \, U_2 \qquad\qquad (37)$$

The boundary conditions for k and ϵ are also related to the friction or shear velocity U_* and are given by Equations 36 and 35, respectively, where z in the ϵ equation is now given by $z = z_1$. These boundary conditions can also be obtained by noting that in the region near the wall the Reynolds stresses are nearly constant (Rodi, 1984). Here convection and diffusion is small and the production due to shear and viscous dissipation terms are balanced.

For the particle concentration equation the horizontal surface boundary condition can be obtained by applying the concentration equation at that surface. Since the only diffusion influence present there is due to the viscosity of the fluid, and the only convective component existing is due to the particle settling velocity, the equation reduces to the boundary condition stated above. For the case of vertical surfaces, since both convective and diffusive processes are negligible or nonexistent there, the concentration there cannot rise above zero.

Model Summary

Combining the above information yields the coupled, highly non-linear system of equations which models the steady state, two-phase, two-dimensional turbulent flow field. The system of equations is found in Figure 2.

Application of this model is restricted to particulate volume fractions $\theta = \rho_p/\rho_s$ of order 10^{-3} or less. Since the solid material density of an ice grain $\rho_s = 910 \text{ kg/m}^3$, the particulate phase density cannot be greater than order 1. With a fluid phase density $\rho = 1.29 \text{ kg/m}^3$, this corresponds to the restriction that the particulate concentration $w = \rho_p/\rho$ must be of order ≤ 1. This criterion is easily met in both blowing snow and precipitating snow storms. For example, consider a snow storm with a moderate to high snow accumulation rate of 2 cm/hr, a snow settling velocity of 0.75 m/s, and a snow accumulation density of 200 kg/m^3. Here $w = \rho_p/\rho = 0.001$, which is still three orders of magnitude less than required by the above restriction. In the case of blowing and drifting snow, Budd et al. (1966) showed the criterion to be satisfied above 1 cm in the saltation layer. Also, extrapolation of data presented by Schmidt (1982b) suggests similar results.

$$\frac{\partial U}{\partial x} + \frac{\partial V}{\partial z} = 0 \qquad (38)$$

$$U\frac{\partial U}{\partial x} + V\frac{\partial U}{\partial z} = -\frac{1}{\rho}\frac{\partial P}{\partial x} + \frac{\partial}{\partial x}\left(\left(c_\mu\frac{k^2}{\epsilon}\right)\frac{\partial U}{\partial x}\right) + \frac{\partial}{\partial z}\left(\left(c_\mu\frac{k^2}{\epsilon}\right)\frac{\partial U}{\partial z}\right) \quad (39)$$

$$U\frac{\partial V}{\partial x} + V\frac{\partial V}{\partial z} = -\frac{1}{\rho}\frac{\partial P}{\partial z} + \frac{\partial}{\partial x}\left(\left(c_\mu\frac{k^2}{\epsilon}\right)\frac{\partial V}{\partial x}\right) + \frac{\partial}{\partial z}\left(\left(c_\mu\frac{k^2}{\epsilon}\right)\frac{\partial V}{\partial z}\right) \quad (40)$$

$$U\frac{\partial k}{\partial x} + V\frac{\partial k}{\partial z} = \frac{\partial}{\partial x}\left(\frac{c_\mu}{\sigma_k}\frac{k^2}{\epsilon}\frac{\partial k}{\partial x}\right) + \frac{\partial}{\partial z}\left(\frac{c_\mu}{\sigma_k}\frac{k^2}{\epsilon}\frac{\partial k}{\partial z}\right)$$
$$+ c_\mu\frac{k^2}{\epsilon}\left(\frac{\partial U}{\partial z} - \frac{\partial V}{\partial x}\right)^2 - \epsilon - \frac{2k}{t^*}\left(1 - \exp\left(-0.5\,t^*\frac{\epsilon}{k}\right)\right)w \qquad (41)$$

$$U\frac{\partial \epsilon}{\partial x} + V\frac{\partial \epsilon}{\partial z} = \frac{\partial}{\partial x}\left(\frac{c_\mu}{\sigma_\epsilon}\frac{k^2}{\epsilon}\frac{\partial \epsilon}{\partial x}\right) + \frac{\partial}{\partial z}\left(\frac{c_\mu}{\sigma_\epsilon}\frac{k^2}{\epsilon}\frac{\partial \epsilon}{\partial z}\right)$$
$$+ c_{1\epsilon}c_\mu k\left(\frac{\partial U}{\partial z} - \frac{\partial V}{\partial x}\right)^2 - c_{2\epsilon}\frac{\epsilon^2}{k} - \frac{2\epsilon}{t^*}w \qquad (42)$$

$$U\frac{\partial w}{\partial x} + (V - V_s)\frac{\partial w}{\partial z} = \frac{\partial}{\partial x}\left(\frac{c_\mu}{\sigma_t}\frac{k^2}{\epsilon}\frac{\partial w}{\partial x}\right) + \frac{\partial}{\partial z}\left(\frac{c_\mu}{\sigma_t}\frac{k^2}{\epsilon}\frac{\partial w}{\partial z}\right) \qquad (43)$$

Figure 2. The system of partial differential equations which models the steady state, two-phase, two-dimensional turbulent flow field.

CHAPTER 5

COMPUTATIONAL APPROACH TO MODEL SOLUTION

The six equation model presented in Figure 2 represents an imposing system of coupled partial differential equations. Any solution of the full steady or unsteady Navier-Stokes equations which includes a turbulence model is a formidable task, as illustrated by the following quote taken from ASCE (1988):

> The development of such a code is typically the result of teamwork by research groups at universities, specialized laboratories or institutes. A typical team working on the development of a turbulence model-based code may consist of two or more senior researchers, two or more junior researchers, and often graduate students.... The duration of a code development project may be from two to four years.

In light of this, an existing algorithm was implemented and modified to fit the requirements of this particular problem. The SIMPLER finite control volume algorithm described by Patankar (1980) was used to solve the continuity, x and z momentum, k and ϵ turbulence, and particle concentration equations. Since the details of

Patankar's computational scheme is well documented in
his 1980 book, only a broad outline of the method will
be presented here. In addition, problem specific
modifications and implementations will be discussed.

The SIMPLER acronym stands for Semi-Implicit Method
for Pressure-Linked Equations, Revised. The term semi-
implicit refers to the method by which a pressure
correction is related to a correction of the velocity as
the solution progresses. In the Navier-Stokes
equations, if the correct pressure field is given, then
solving the momentum equations will lead to velocities
which satisfy the continuity equation. Since the
continuity equation is directly related to the pressure,
it can be reformulated into a Poisson equation for
pressure. The goal of the numerical scheme is to
iteratively correct a guessed velocity field in order to
produce a pressure field which is compatible with
continuity. SIMPLER can be thought of as an iterative,
pseudo time dependent formulation in which the
discretized equations are marched from an initial
condition, to the steady state solution. To ensure that
the discretized equations are linear during the current
iteration, some of the coefficients are evaluated at the
previous iteration level. For this specific application
the algorithm consists of the following sequence of

steps:

1)   Provide initial guesses for the U, V, k, ϵ, and w fields.

2)   Compute a psuedo velocity from the momentum equations in the absence of the pressure terms.

3)   Solve a pressure equation for the pressure field.

4)   Using this pressure field, solve the momentum equations for the velocity.

5)   Solve a pressure-correction equation.

6)   Use this pressure-correction information to update the velocities.

7)   Solve the k and ϵ equations using these new velocities.

8)   Solve the concentration w equation using the new values for k and ϵ.

9)   Return to step 2.

SIMPLER and related schemes have been widely tested and are a commonly used approach for solving incompressible viscous flow problems (Fletcher, 1988).

SIMPLER is a second order implicit formulation which is based on the concept of the control volume. The computational domain is divided into a series of control volumes, each of which encloses a grid point.

The differential equation is then integrated over each control volume. This produces the desirable characteristic of coarse grids yielding solutions which represent exact integral balances. The grid spacing can be nonuniform in both the x and z directions. This allows efficient use of computing energy by enabling the user to define course grids in regions where the gradients of the dependent variables are small.

Patankar (1978) introduced a harmonic mean approach to describe the value of the diffusion coefficient (viscosity) at control volume interfaces, based on diffusion coefficient values at the main grid points (control volume centers). This approach, as opposed to using the arithmetic mean, correctly deals with large step changes in the diffusion coefficient from one control volume to another. As an example application, a very large viscous coefficient can be used to force the velocity within a control volume to zero. The use of the harmonic mean ensures that neighboring control volumes consider the velocity throughout that control volume be zero. Effectively the zero velocity has been transferred from the main grid point to the control volume wall. The use of the harmonic mean has been implemented in SIMPLER, and the details are included in Patankar (1980).

To assist in the accurate numerical solution of convection dominated flows, an additional feature of SIMPLER is the use of a weighted upwinding scheme where the degree of upwinding imposed at each grid point depends on the ratio of the strengths of convection to diffusion. Applying central differences to convection dominated convection-diffusion problems can lead to physically unrealistic results. This can generally be attributed to the formation of negative coefficients (Patankar, 1980). Although this can be remedied by refining the grid spacing, it is much more desirable to develop a scheme which produces reasonable results using course grids. General upwinding at all grid points would be one solution to the problem, but in applications containing some regions not dominated by convection this would not be an acceptable practice. Patankar's approach is to compute the relative influences of convection and diffusion, and then weight the degree of upwinding accordingly. An additional concern which must be accounted for is that the scheme must be able to identify which direction is upwind, since in complex flows with flow reversals this may vary throughout the domain.

Application to the Turbulent Flow Model

To bring the model and associated boundary conditions to solution, several problem specific factors must be addressed. In this section such concerns as source term linearization, underrelaxation of the solution evolution, and declaring convergence will be discussed.

Implementation of the SIMPLER algorithm leads to a fully implicit system of linear algebraic equations for each discretized partial differential equation solved. Since two-dimensional problems lead to sparse systems containing five diagonal sequences of coefficients, considerable computer storage can be consumed by nonessential zeros in the systems of equations if they are stored in standard matrix form. To alleviate this problem a sparse storage scheme has been implemented which stores only the necessary coefficients and an index value describing their original positions, for each system of equations. Each of these systems is solved during every global iteration cycle. The Thomas algorithm (Anderson et al., 1984) is used to solve the systems of equations. This is a highly efficient direct solver for tridiagonal systems of equations found in one-dimensional problems. To apply the Thomas algorithm

to the two-dimensional problems of interest in this study, a grid line is chosen in the x or z direction and the dependent variable is assumed known, from their latest values, at the grid lines on either side. The algorithm can then be used to solve for the dependent variables along that center line. In the solution implementation this iterative, line-by-line method is first used to sweep through the domain in the x and then the z direction, completing one iteration. The iterations are repeated until the maximum absolute difference between successive iterations is less than some set tolerance. If the x direction sweep is made in the direction of the main flow, a tolerance of 10^{-6} is typically achieved in fewer than seven iterations for all equations except the one for pressure.

Ferziger (1990) noted that it is typical for incompressible viscous flow solution schemes to spend the majority of their computing time solving the pressure equation. Since it is only the pressure differences which are meaningful in these applications, not the absolute value of pressure, it is common to apply a normal pressure derivative equal to zero condition to all flow domain boundaries. This implies that the pressure field and the pressure field plus any arbitrary constant are satisfactory solutions to the

pressure equation. In this case a direct solution method would indicate a singular system of equations, while an iterative method like the Thomas line-by-line method will actually converge to a pressure field which marches by a constant at each subsequent iteration.

The nonlinear source terms in the partial differential equations for k and ϵ must be linearized, and this linearization must ensure that the dependent variables k and ϵ are always positive. This positive status is critical for both physical realism and numerical stability. To implement the linearization, the source terms S are cast in the form

$$S = S_c + S_\phi \phi \qquad (44)$$

where S_c is the constant part of S, and S_ϕ is the coefficient of the dependent variable ϕ. For the case where the dependent variable is not required to be positive, the S_ϕ term must be negative or zero. Again this is required for physical reality and computational stability. For always positive variables, a positive or zero S_c is an additional requirement (Patankar, 1980).

To place S in this form, one desirable approach is to expand nonlinear terms in a Taylor series about the value of the dependent variable at the previous iteration, and keep the first two terms. This leads to